ISTITUTO NAZIONALE DI FISICA NUCLEARE

Sezione di Milano

INFN/TC-02/27
12 Dicembre 2002

BEHAVIOUR AND MEASUREMENTS OF THE INTERPANCAKE JOINT OF THE B0 ATLAS MODEL COIL

Francesco Broggi[1], Nello Dolgetta[2], Giovanni Volpini[1]

[1)] INFN-Sezione di Milano Laboratorio LASA, Dipartimento di Fisica dell'Università degli Studi di Milano, via fratelli Cervi 201, 20090 Segrate MI, Italy
[2)] Euratom-DRFC-CEA Cadarache St Paul Les Durance 13108 France

Abstract

The ATLAS Barrel Toroid (BT) consists of 8 superconducting coils of 25 m length and 5 m width, it provides the magnetic field for the muon spectrometer of the ATLAS detector, one of the experiments of the Large Hadron Collider, under construction at CERN. The cable used for the coils is an Aluminum stabilized NbTi rutherford cable and the coils are built with the double pancake technique, so a resistive joint between the cables of the two single pancake is present. The transverse magnetic field induces eddy currents, during the ramping of the main current, whose intensity can sometimes exceed the transition limit. B0 is a one third length, full large scale model of one of the eight magnet composing the ATLAS barrel toroid. The B0 construction was decided to test the technical construction solutions and reproduce the behaviour of the final coils.

In this paper the behaviour of the interpancake joint is analyzed and compared with theoretical models describing the current distribution at the joint. Measurements of the joint resistance are reported.

PACS.: 73.40.-c

*Published by **SIS–Pubblicazioni***
Laboratori Nazionali di Frascati

1 INTRODUCTION

The Barrel Toroid Magnet (BT)[1)] is part of the Magnet System of the ATLAS Detector for the Large Hadron Collider (LHC). It provides the magnetic field required by the muon spectrometer. It consists of eight flat superconducting coil of 25 m length and 5 m width, radially assembled around the beam axis.

The field will extend over a length of about 26 meters with an inner bore of 9 meters and an outer diameter of about 20 meters. Because these coils are about 5 times larger than any other superconducting coil ever built, the CEA (Saclay), CERN and INFN (Milan) decided to build a working model, called B0, which will be similar to one BT coil, both for the design concept and the construction procedure with the same width and the same cross section (4.5 m x 0.3 m) but with a reduced length (9 m), in order to qualify the design, verify the manufacturing procedure and validate the technical solutions.

The B0 coil in the test station at CERN is shown in Fig. 1.

FIG. 1 – The B0 model coil in the test station at CERN.

The cable used for the magnet coil is an Al stabilized NbTi rutherford cable. The main characteristics of the cable are listed in Table 1.

TABLE 1 – BT/B0 cable characteristics

Conductor cross section	57 mm x 12 mm
Rutherford cross section	26 mm x 2.3 mm
RRR of Aluminum matrix (B = 0 T)	>1000
Critical Current (T = 4.2. K; B = 5 T)	> 58 kA

The coils are wounded with the double pancake technique, so a resistive joint is present between them.

Because of the joint position, outside the symmetry plane, a transversal magnetic field is present so eddy currents arise during the ramping of the main current, whose intensity can be of the order of some tens of kiloamps, reaching the transition limit.

In this paper the field at the joint is evaluated in order to have an exact estimation of the eddy current induced, then the measurements of the joint resistance are presented, together with the eddy current measurements, obtained with hall probes facing the joints, during the B0 tests. The data are then compared with theoretical models describing the joints.

2 MAGNETIC FIELD AT THE JOINT

Each of the eight BT, and the B0 coil too, is composed by two double pancakes, so the interpancake joint is outside the median plane, as a consequence a transverse field is present at the joint. In Fig. 2 the geometry of the cables of the two double pancake is shown together with a vector graph of the magnetic field. The vector graph is only qualitative giving the direction of the magnetic field, but not the magnitude, being the vector length not proportional to the magnitude.

The magnitudes of the magnetic field components, evaluated with an ad hoc Biot-Savart code and using Microcal™ Origin™ graphic package are plotted in Fig 3 and 4.

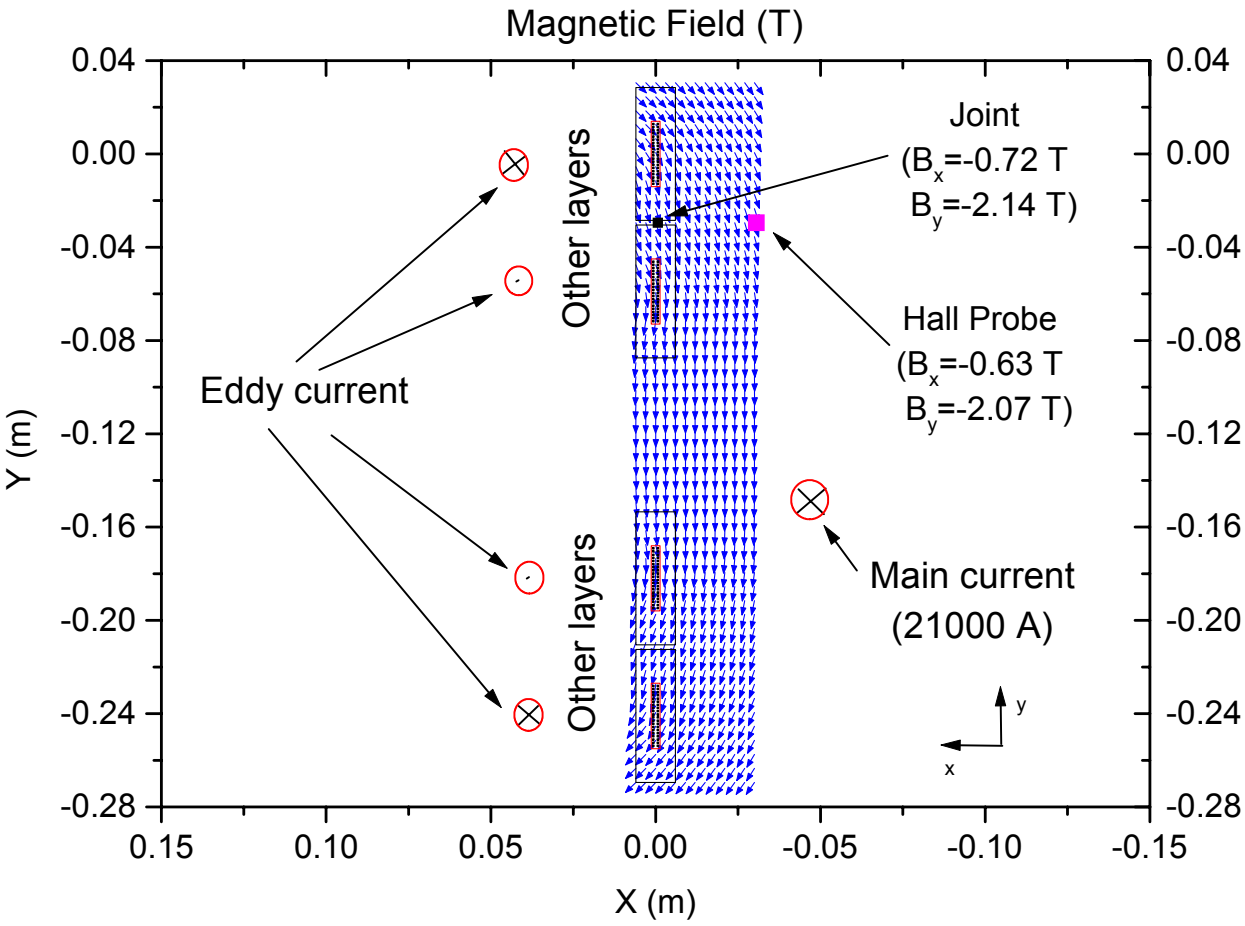

FIG. 2 – Scheme of the coil cable geometry and qualitative vector plot of the magnetic field at the joint and at the position of the Hall Probe. (The length of the vectors is not proportional to the field magnitude).

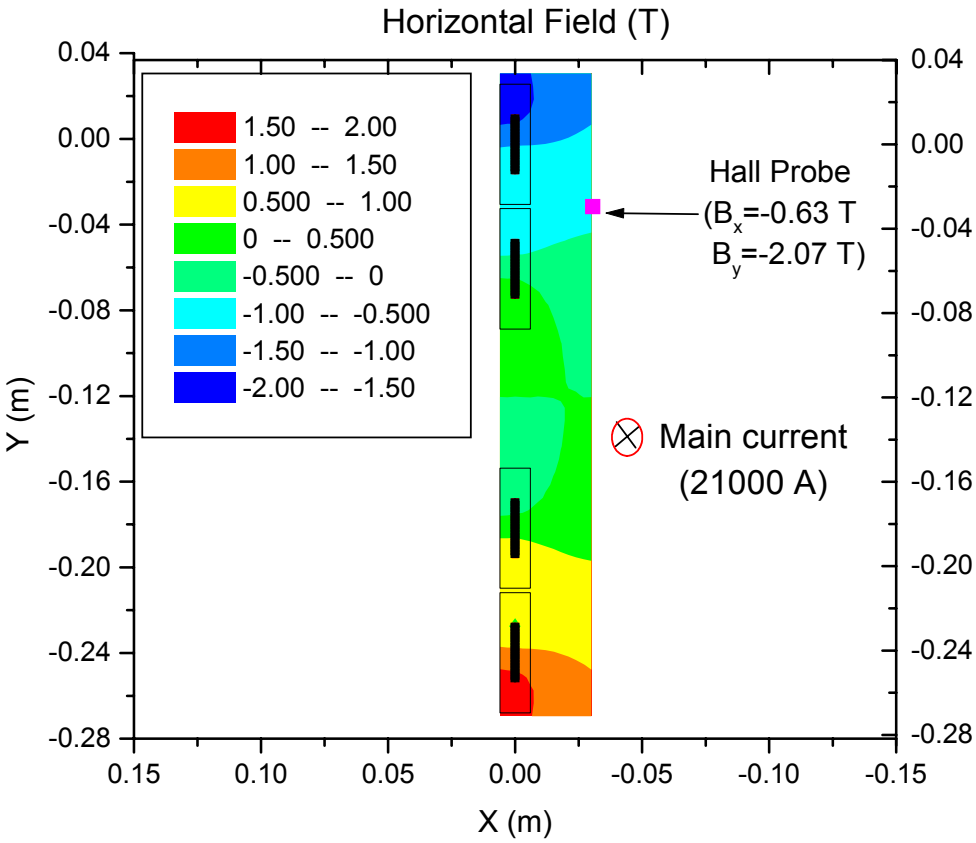

FIG. 3 – Horizontal field map

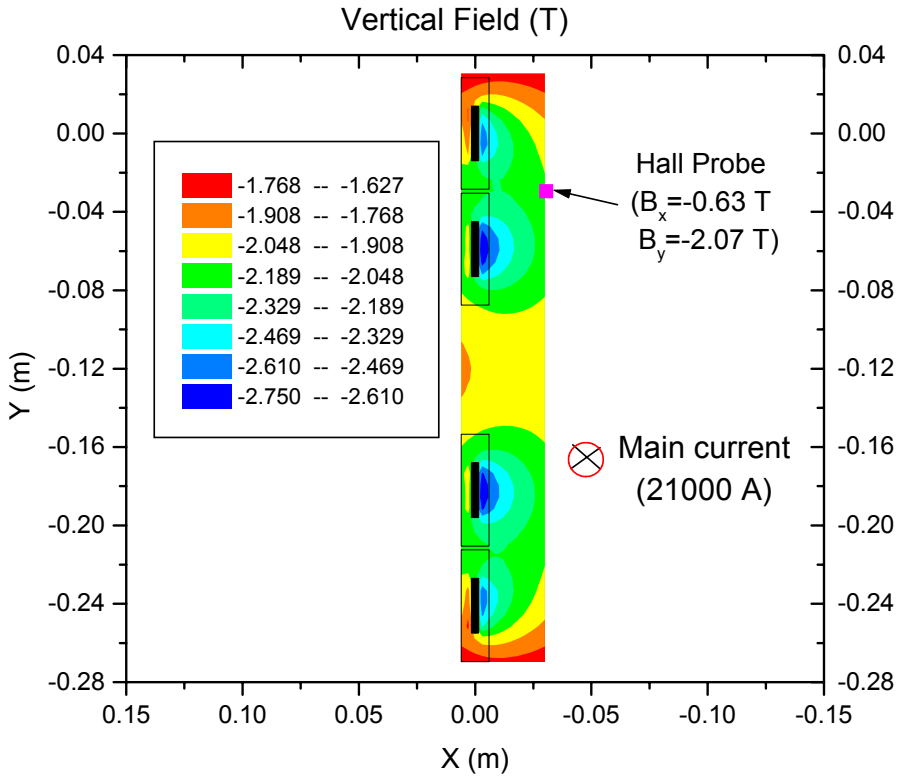

FIG. 4 – Vertical field map

3 MEASUREMENTS OF THE JOINT RESISTANCE

Being B0 a prototype coil, many sensors are installed on it[2], in order to verify and fully monitor each part of the magnet.

For the joint monitoring, voltage taps and Hall probes are used.

Each interpancake joint is equipped with a pair of voltage taps, to measure and monitor the voltage drop across the joint, and with two Hall probes, to measure the intensity of the eddy currents.

The Hall probes are placed at ½ and ¼ of the joint length. These sensors are connected to the acquisition system of the electrical quantities[3].

The resolution of the acquisition system and the noise due to the long cables connecting the B0 magnet with the acquisition system (~100 m) do not allow accurate measurements of the voltage across the joint (some μV), so a dedicated instrument has been used.

The voltage taps were directly connected to an HP 34420A multimeter, as close as possible to B0 (~15 m). The voltage drop across the joint has been recorded during the step excitation of the coil.

The data are shown in Fig.5.

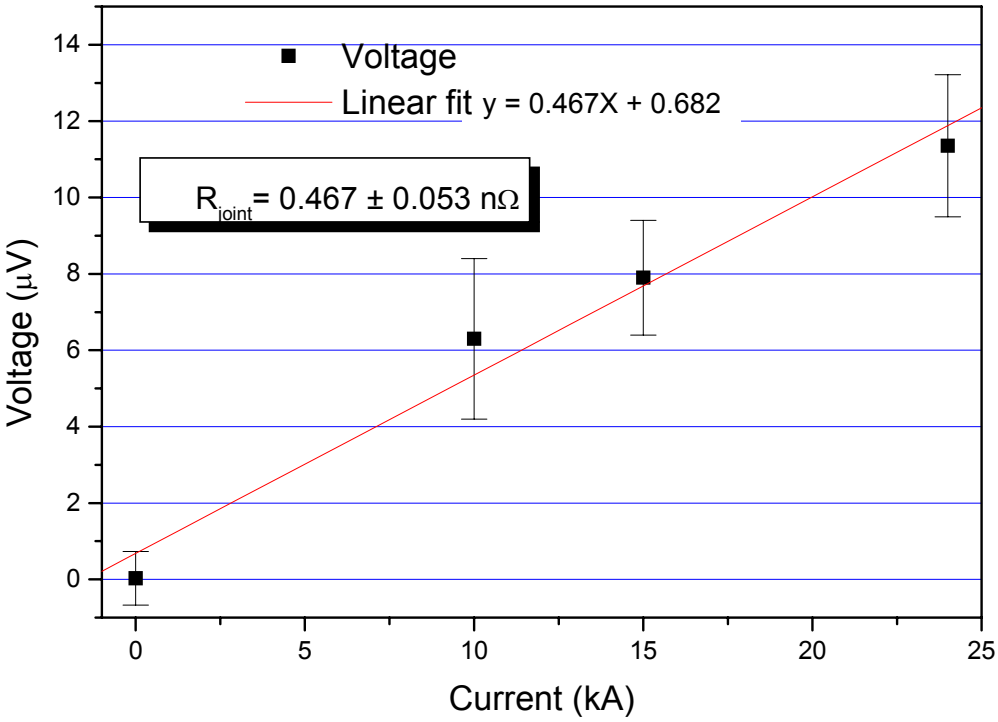

FIG. 5 – Joint resistance measurements.

As we can see, assuming a linear dependence between the voltage and the current, a value of the interpancake joint resistance of 0.47 ± 0.05 nΩ follows.

The joint resistance can be splitted in two terms:

$$R_j = R_{mat} + R_{mech} \tag{1}$$

where R_{mat} is the resistance due to the Al characteristics and to the geometry of the junction of the cable while R_{mech} is the resistance of the junction welding between the two cables.

From the geometry of the joint (see Fig. 6), the characteristic of the Aluminum and the measured resistance we can evaluate the contact resistance of the joint (R_{mech}).

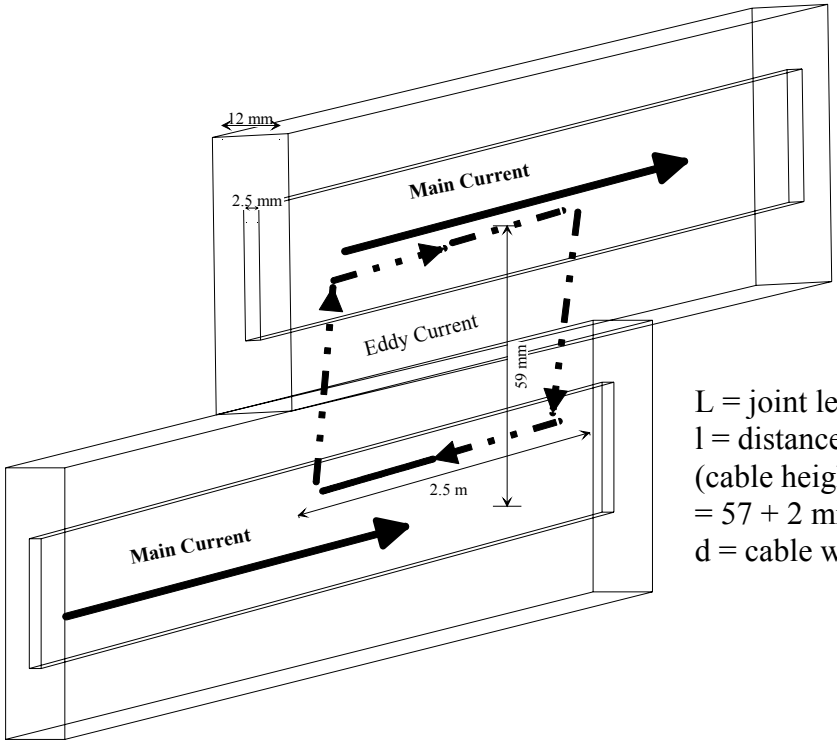

L = joint length = 2.5 m
l = distance between the two insert (cable height + insulation distance) = 57 + 2 mm = 59 mm
d = cable width = 12 mm

FIG. 6 – Scheme of the joint.

We have $R_{mat} = \rho l/S$ with $\rho = \rho_{Al}/RRR$ where ρ_{Al} is the resistivity of the Aluminum and RRR is the residual resistivity ratio, taking into account of the magnetoresistive effect.

Unfortunately, because of the very low level of the signals, we do not have measurements below 10 kA, where most of the magnetoresistive effect occurs.

For this reason we can have a good estimation of R_{mat} and R_{mech} by considering the values at full current.

Follows:

$$R_{mat} = \rho \frac{l}{S} = \rho \frac{l}{Ld} = \frac{2.7 \times 10^{-8}}{420} \frac{59 \times 10^{-3}}{2.5 \cdot 12 \times 10^{-3}} = 0.126\,\text{n}\Omega \tag{2}$$

For the R_{mech} term we get

$$R_{mech} = 0.467 - 0.126 = 0.341\,\text{n}\Omega. \tag{3}$$

4 EDDY CURRENTS

The geometry of the magnet, with the joint outside the median plane gives an horizontal component of the magnetic field. During the ramping up/down of the main current this field variation induces eddy currents in the joint whose amplitude varies exponentially with a characteristic time constant τ. From the resistance data and the geometry of the junction a theoretical evaluation of the eddy current can be done. Let' s determine the order of magnitude of the eddy current by elementary consideration.

The inductance of the joint is $1.458 \text{x} 10^{-6}$ H while the electromotive force is given by the time variation of the flux of the horizontal magnetic field component, linked with the section of the joint, i.e.

$$V_{eddy} = S \frac{dB}{dt} = L \cdot l \frac{dB}{dt} = L \cdot l \cdot K_{main} \frac{dI_{main}}{dt} \tag{4}$$

With

$$K_{main} = \frac{B_x}{I_{main}} = 3.42 \times 10^{-5} \frac{\text{T}}{\text{A}} \tag{5}$$

where K_{main} is the proportional coefficient between the horizontal magnetic field at the joint and the main current.

Considering an uniform field across all the junction section and a ramp rate of the main current of about 10 A/s, from (4) a value of about 50 μV for the electromotive force follows; dividing by two times the resistance (the resistance of the eddy current loop) we get a value of about 50 kA for the eddy current.

At first sight very high value must be expected, probably exceeding the critical current value. For this reason a good evaluation of the behaviour of the joint must be done during the magnet design, in order to have a precise evaluation of the safety operation margin of the magnet.

The simplest way to evaluate the eddy current is to consider the joint as a resistor-inductance circuit while the current generator is the magnetic field flux variation. A more sophisticated model is reported in[4]; according to this model the junction is represented as a resistor-inductance network, and the eddy current distribution in the joint can be derived.

5 B0 TESTS

Here the experimental data got during the test on the B0 model coil are reported. They are the signals form the Hall probes facing the joints. Two hall probes (MME031 and MME032) are placed on the upper double pancake, the former are ½ length the latter at ¼ length), two more hall probes (MME033 and MME034) face the joint of the lower double pancake.(MME033 at ½ length, and MME034 at ¼ length).

5.1 Current ramp up

The data of the four Hall probes during a charging of the magnet up to 21 kA with a ramp rate of 15 A/s are shown in Fig. 7.

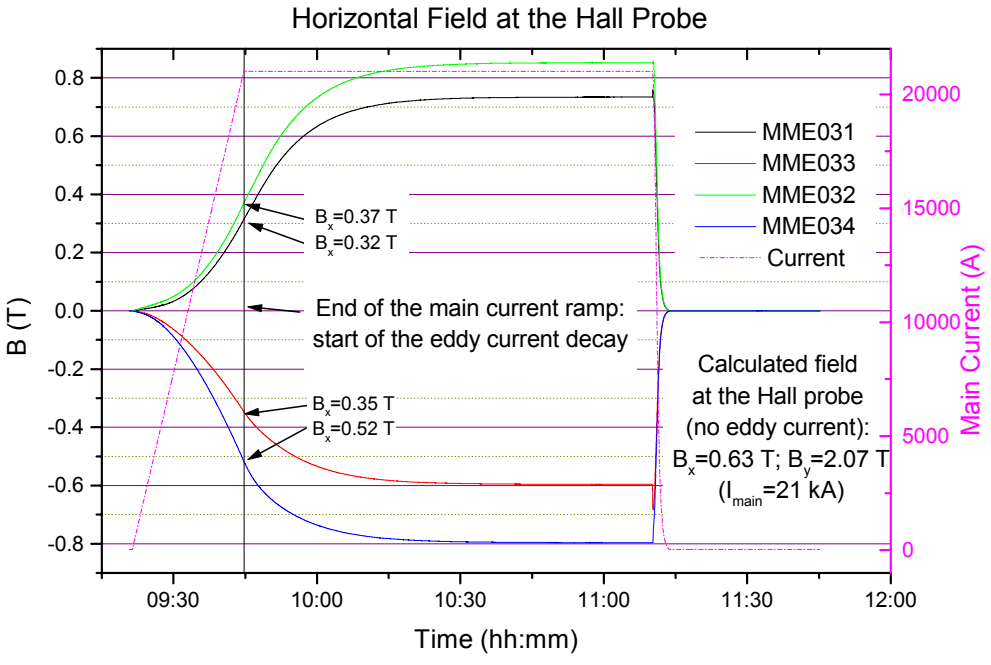

FIG. 7 – Hall probe data during a 15 A/s ramp up of the main current (I_{max} = 21 kA).

The calculated magnetic field at the Hall probe position is $B_x = 0.63$ T and $B_y = 2.07$ T (as already shown in Fig. 2).

The same calculation used to determine the magnetic field at the Hall probe position (HP) and at the joint can be done for the eddy currents. For a main current of 21 kA and eddy current of 50 kA the same calculation gives the results shown in Table 2.

TABLE 2 – Horizontal field and K value (proportional constant between the horizontal field and the current) for 21 kA main current and 50 kA eddy current at the Hall Probe (HP) and at the joint.

	B_x (at HP)	K(at HP)	B_x (at joint)	K(at joint)
I_{main}	0.630	3.0×10^{-5}	0.718	3.42×10^{-5}
I_{eddy}	0.337	6.733×10^{-6}	0.764	1.53×10^{-5}

Being:

$$B = K_{main} I_{main} + K_{eddy} I_{eddy} \tag{6}$$

from the data above, scaling to the values to the experimental data, we can get the value of the eddy current.

The measured horizontal field component at the end of the ramp (when the eddy current are at their maximum) and at steady state (no eddy current) and the amplitude of the eddy current, as from (6), are shown in Table 3.

TABLE 3 – Measured horizontal component of the magnetic field at the end of the ramp (maximum eddy current) and at steady state (no eddy current).

	MME031	MME032	MME033	MME034
B_x (stady state)	0.734	0.853	0.596	0.797
B_x (end of ramp)	0.315	0.371	0.347	0.518
I_{eddy}	~ 46700	~ 38400	~ 42000	~ 16700

As we can see the amplitude of the eddy current is about 40-50 kA. The even Hall probes measure lower currents, because of the current distribution inside the joint; the discrepancy between these two sensors may be due to different sensitivity of the sensors (especially for MME034).

As a matter of fact we did not performed any calibration on these sensors, but have only the factory nominal characteristics.

The total current in the joint is given by the main current I_{main} and the eddy current I_{eddy}.

$$I_J = I_{main} + I_{eddy} \tag{5}$$

The time dependence of the eddy current decay (after the end of the main current ramp) can be described by an exponential function

$$I_J(t) = I_\infty + (I_0 - I_\infty) \cdot e^{-t/\tau(t)} \tag{6}$$

where I_∞ is the current value when the eddy current are decayed (i.e. the main current) and I_0 is the current when the ramp is stopped (at t=0), and τ is the characteristic time eddy current behaviour, usually referred as a "time constant".

Because of the magnetoresistive effect, the resistance of the joint is not constant during the decay of the eddy current, as a consequence the time constant varies.

From eq. (6) the time constant is given by :

$$\tau(t) = -\frac{t}{\ln\left(\frac{I(t) - I_\infty}{I_0 - I_\infty}\right)} \tag{7}$$

The time variation of the time constant after the ramp up of the main current, as calculated from (7) is shown in Fig. 8.

To evaluate the time constant we can follow two methods.

- Evaluate at what time the eddy current is decayed of 1/e.
- Evaluate when the eddy current is decayed of 90 % (arbitrary figure) and then average over this time the values of the time constant.

The first method gives the time constant at the beginning of the eddy current discharge, while the second one provides a time averaged of the eddy current characteristic time.

The evaluation of the time constant for both methods is shown in Table 4.

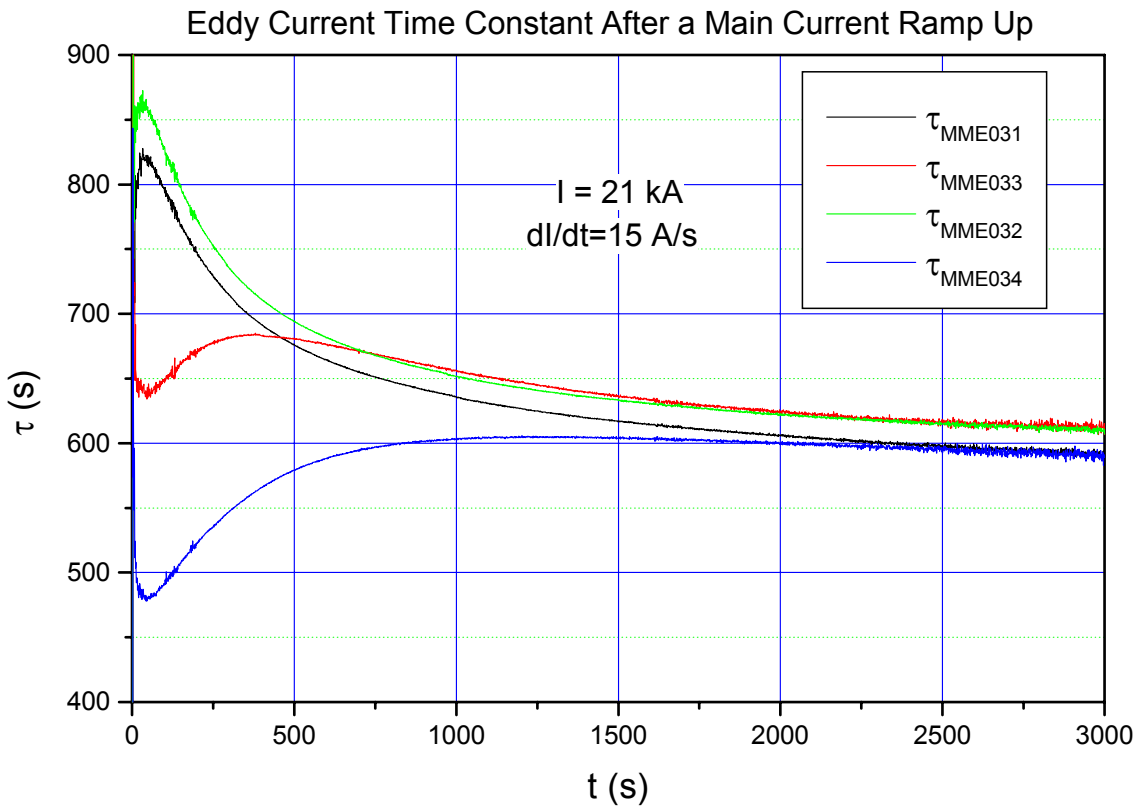

FIG. 8 – Time dependence of the eddy current time constant.

TABLE 4 – Time constant τ_B of the eddy current decay after a ramp up of the main current to 21 kA with a ramp rate of 15 A/s.

	MME031	MME032	MME033	MME034
τ (first method)	658	674	673	587
τ (second method)	674.6 ± 55.2	693.3 ± 61.8	662.1 ± 17.1	575.6 ± 37.7

From the table above a mean value of about 648 ± 36 s, for the first method and 651 ± 93 follows.

Let' s note once again the discrepancy of the MME034 sensor, respect to the others.

Neglecting the MME034 value a time constant of 668 ± 7 s and 677 ± 85 follows.

5.2 Current ramp down

The data of the four Hall probes during a slow discharge of the magnet from 20.5 kA are shown in Fig. 9.

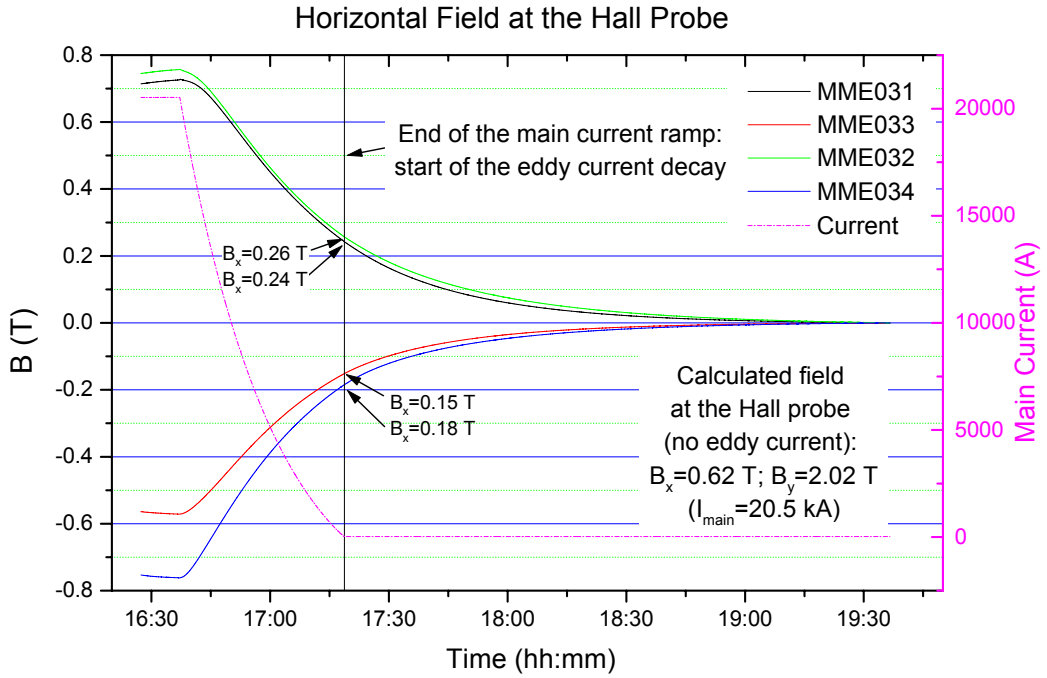

FIG. 9 – Hall probe data during a slow discharge of the main current (I_{max} = 20.5 kA).

During the magnet discharge the eddy current increase their amplitude and reach their maximum when the main current is zero. Again we can evaluate the amplitude of the eddy current as for the current ramp up. The data are shown in Table 5.

TABLE 5 – Measured horizontal component of the magnetic field at the end of the discharge (maximum eddy current).

	MME031	MME032	MME033	MME034
B_x	0.242	0.257	0.151	0.184
I_{eddy}	~ 36000	~ 38000	~ 22500	~ 27400

The time constant of the current in this case is higher than in case of ramping up of the current because of the magnetoresistance.

As a matter of fact the resistance now is about a factor 3 lower[5,6], the time constant increases consequently of the same factor.

The total current in the joint is, from (6):

$$I_J(t) = I_0 \cdot e^{-t/\tau(t)} \tag{8}$$

Like in the case of magnet charge, the resistance, and consequently the characteristic time is not constant during the magnet discharge.

This fact is shown in Fig. 10, where the time constant value during the discharge is plotted.

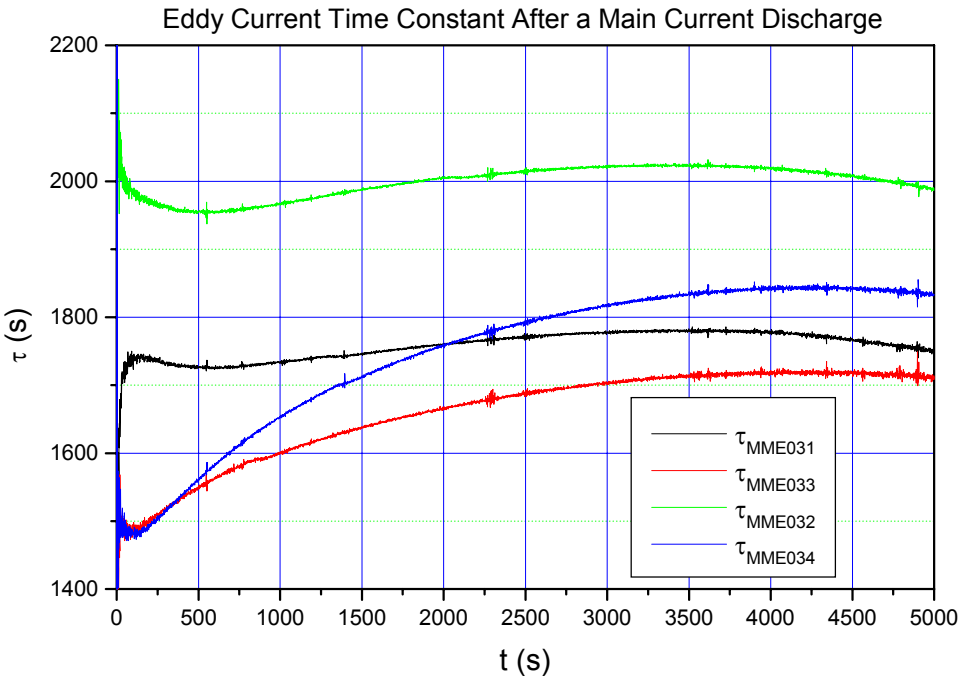

FIG. 10 – Characteristic time of the eddy current during the magnet discharge.

As in the case of the magnet charge we can evaluate the time constant with two methods.

The time constant evaluation is reported in Table 6.

TABLE 6 – Time constant of the eddy current after a slow discharge (I_{max} = 20.5 kA).

	MME031	MME032	MME033	MME034
τ (first method)	1753	2004	1647	1737
τ (second method)	1755.8 ± 29.6	1999.3 ± 24.3	1643.7 ± 68.7	1730.4 ± 109.6

In this case we do not have strange values from the MME034 probe, but the most spreading value comes from MME032.

From the data of the Table 5 a mean value of 1785 ± 133 and 1782 ± 135 s from the second method is obtained for the time constant.

The ratio between the two time constant, the one related to the magnet charge and the one of the magnet discharge is 2.75 ± 0.26 or 2.64 ± 0.39, depending on which of the τ_B is considered; anyway it is good in agreement with the measured residual resistivity ratio of the cable without and with magnetic field[5,6] (1362 ± 14/420± 14 = 3.24 ± 0.11).

5.2.1 Odd voltage discharge

The voltage across the joint was measured by a couple of voltage taps on each joint, but, because of the low signal level (about 10 μV at full current), the signal was not accurately measured by the acquisition system[3], we had only a qualitatively trend.

However during the current discharge some "strange" behaviour was observed at the joint between the pancakes of the DPC1[2], as shown in the lower graph of Fig .11.

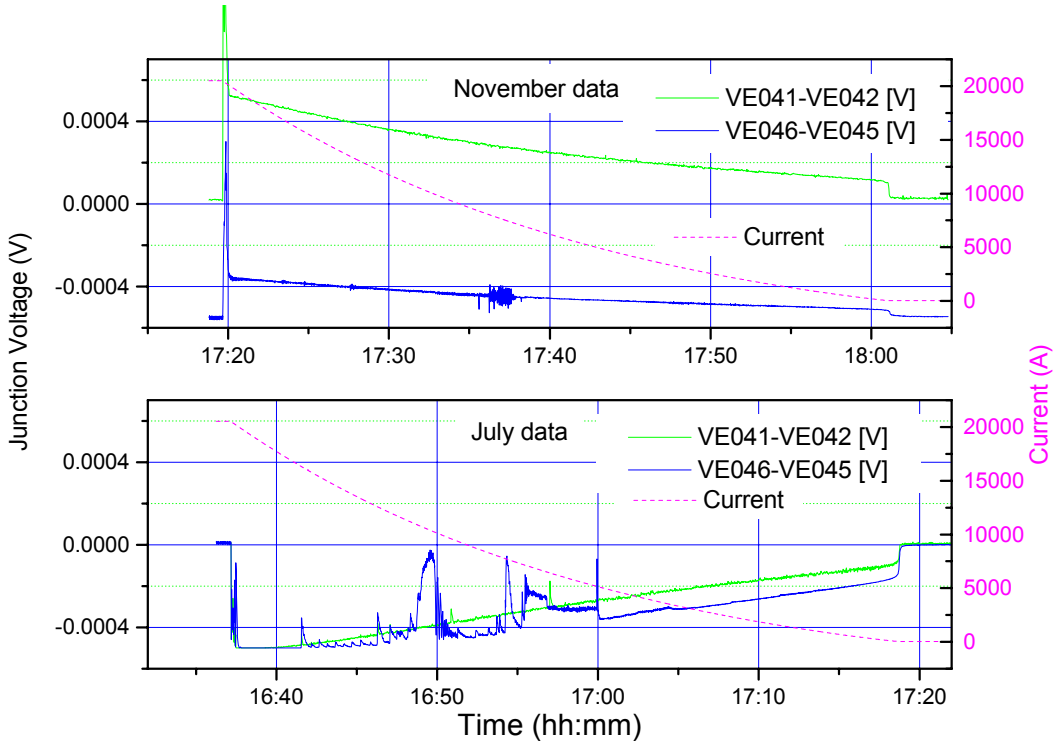

FIG. 11 – Joint voltage during the magnet discharge.

During the current discharge a negative voltage appears, because of the joint inductance. Then a resistive voltage adds to the inductive one, showing a sort of quench inside the joint (at about 16:40 to 17:00). At first sight this can be due to the eddy current that, composed with the main current, exceed the critical value, the transition was then quickly recovered by the stabilizer. This phenomenon repeated systematically at every slow discharge of the magnet at the same value of the main current.

However, after the summer stop, the phenomenon was not present anymore (see Fig. 11, top graph), so was it real or a sort of "noise"? Some reason lead to consider it as a real thing, other drive us to the conclusion that the phenomenon was not real.

In Table 7 the different argumentation are summarized.

TAB. 7: Real or "noise" effect the quench in the joint during the magnet discharge ?

REAL	**"NOISE"**
High repeatability of the effect during the July tests	In November was not present anymore
-	In November no junction voltage was measurable
Damaging of the voltage taps between July and November ?	No effect on the Hall probes signals

The fact that no indication came from the Hall Probes, lead us to the conclusion that the phenomenon is not real.

5.3 Quench

The data of the four Hall probes during a quench is shown in Fig. 12.

In the upper part of the figure the signal of the four Hall probe is shown as recorded from the so-called "slow acquisition", where the sampling time is 1 sec. In the lower part the time amplification around the quench detection trigger, (the window shown in the upper graph) as recorded from the "fast acquisition" is shown[3)]; the main current is shown too (on right scale).

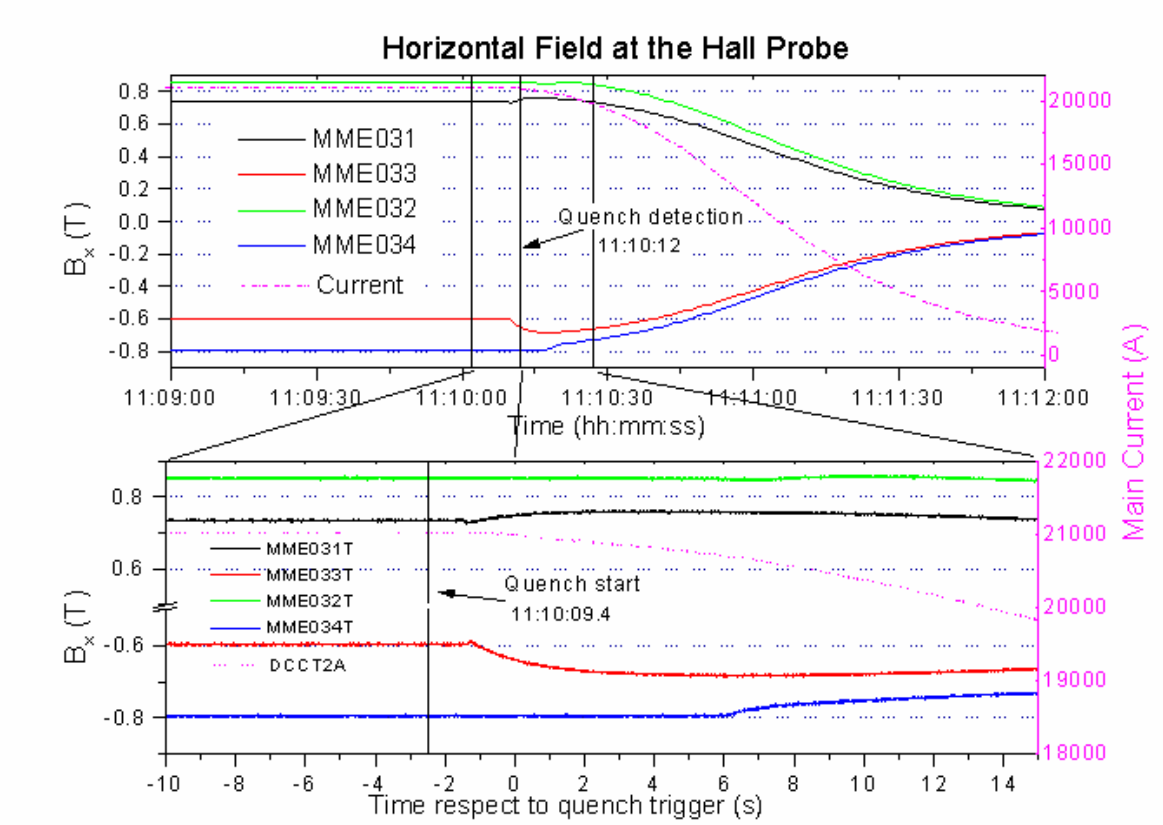

FIG. 12 – Hall probe signal during a quench. Top: "slow acquisition" bottom: "fast acquisition".

As we can see there is an indication of the quench event in the Hall Probe, more evident in the signal from MME031 and MME033.

A magnification of the signal from MME031 is shown in the upper part of Fig 13, in the lower part the signal from a pick-up coil[2,7] is shown.

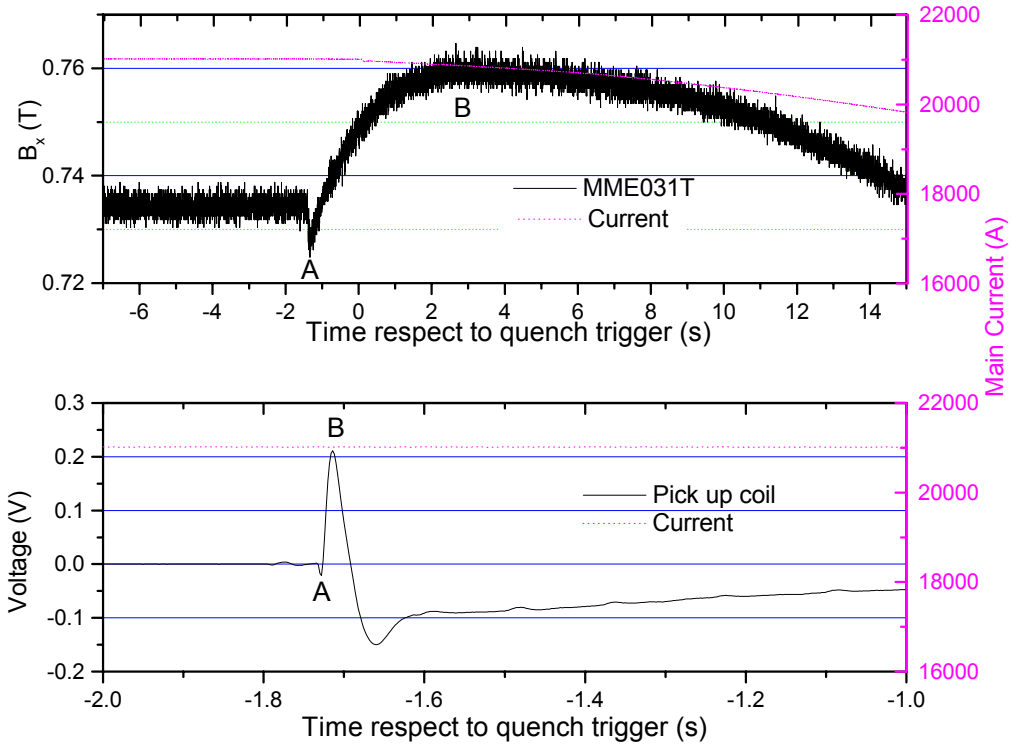

FIG. 13 – Detail of the Hall probe signal (up), pick-up coil signal (down) during a quench.

The time scale of the plot of the Hall probe signal and of the pick-up coil are different because of the different location of the sensor, in addition the time characteristics of the two signal are different, because of the different characteristics of the two sensors, and the different characteristic diffusion time in the two directions. To this aim let's remind that the field measured by the Hall probes is the horizontal field component (x), while the pick-up coils measure the *variation* of the *vertical* field component (y), nevertheless an increase/decrease in the magnitude of the field is reflected in an increase of the field components.

Despite these differences in the two signals some common feature can be found.

At the "beginning" of the event (point A) the x component shows a rapid and small decrease of the field (≈12 mT), then a field increase of about 35 mT follows (point B). This variations cannot be due to breaker opening of to the main current decrease, because the magnet discharge starts at the time "0", and in the upper part of Fig. 11 the field

variation occurs well before the 0 time, in addition the field keep on increasing even after the start of the current discharge (t>0).

The field increase (point B) is due to the current diffusion from the insert to the Al stabilizer along the x direction (the narrow part of the cable), the field decrease at point A is a very rapid phenomenon due to the start-up of the current diffusion (less than 10 ms) from the superconductor and its mechanism is still under study[8].

6 THEORETICAL MODELS

Models describing the joint and the eddy current behaviour has been developed.

In the following the models are described and the results of the calculations are compared with the data reported so far.

6.1 A very simple model

The simplest way to figure out the junction is a resistance-inductance circuit, with a current generator. The joint resistance for the main current is what we measured as in the previous section, while the resistance of the eddy current is twice the measured resistance, because of the current loop.

The inductance of the joint is 1.458 x10^{-6} H; while the electromotive force is given by the time variation of the horizontal magnetic flux, linked with the joint loop area i.e.:

$$V = -\frac{d\phi(B)}{dt} = -S\frac{dB}{dt} = -SK_{main}\frac{dI_{main}}{dT} \tag{9}$$

By solving the circuit equation:

$$L\frac{dI(t)}{dt} + R(I)I(t) = V \tag{10}$$

we have the time evolution of the eddy currents.

The magnetic field evaluated at the Hall probes and the measured field during the ramp up of the current (section 5.1) are shown in Fig. 14. In the upper part of Fig. 14 the eddy current intensity, the main current and their sum is plotted. The calculated and the measured horizontal component of the magnetic field are plotted in the lower part of Fig.14 and 15 (for the magnet charge and discharge respectively). In order to make easier the comparison between the measured and the calculated data, the absolute value of the data of the probe MME033 and MME034 are plotted.

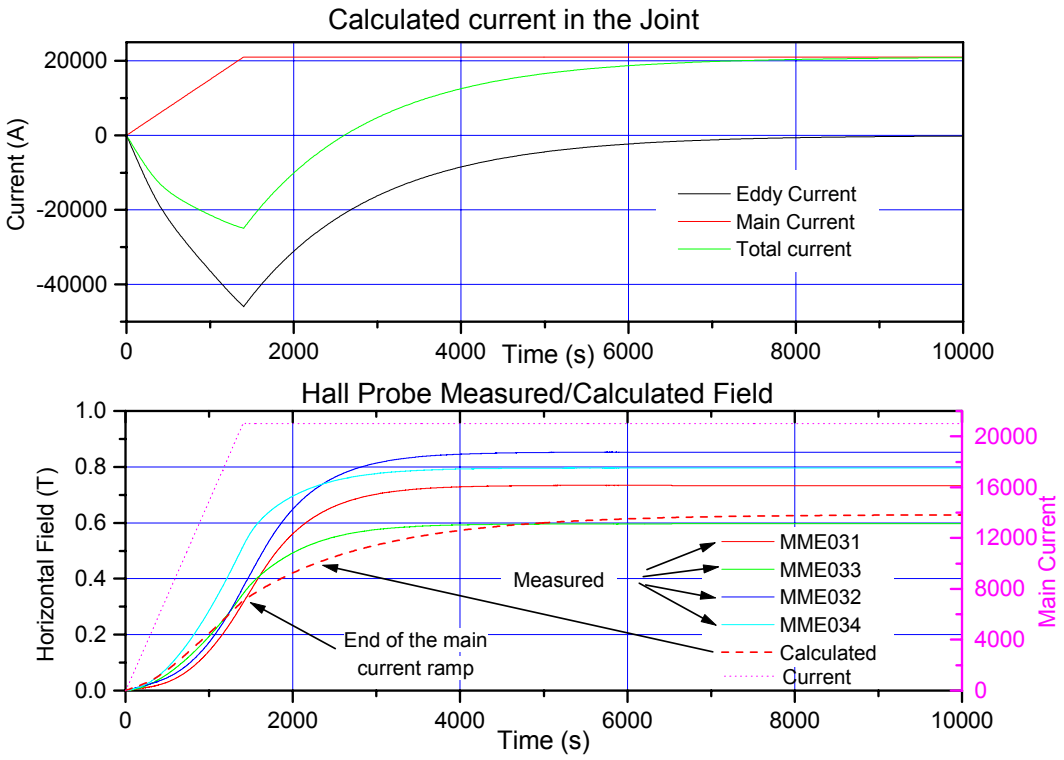

FIG. 14 – Main current, calculated eddy current and total current (top). Measured field (solid lines) and calculated (dotted line) (bottom), during a magnet charge.

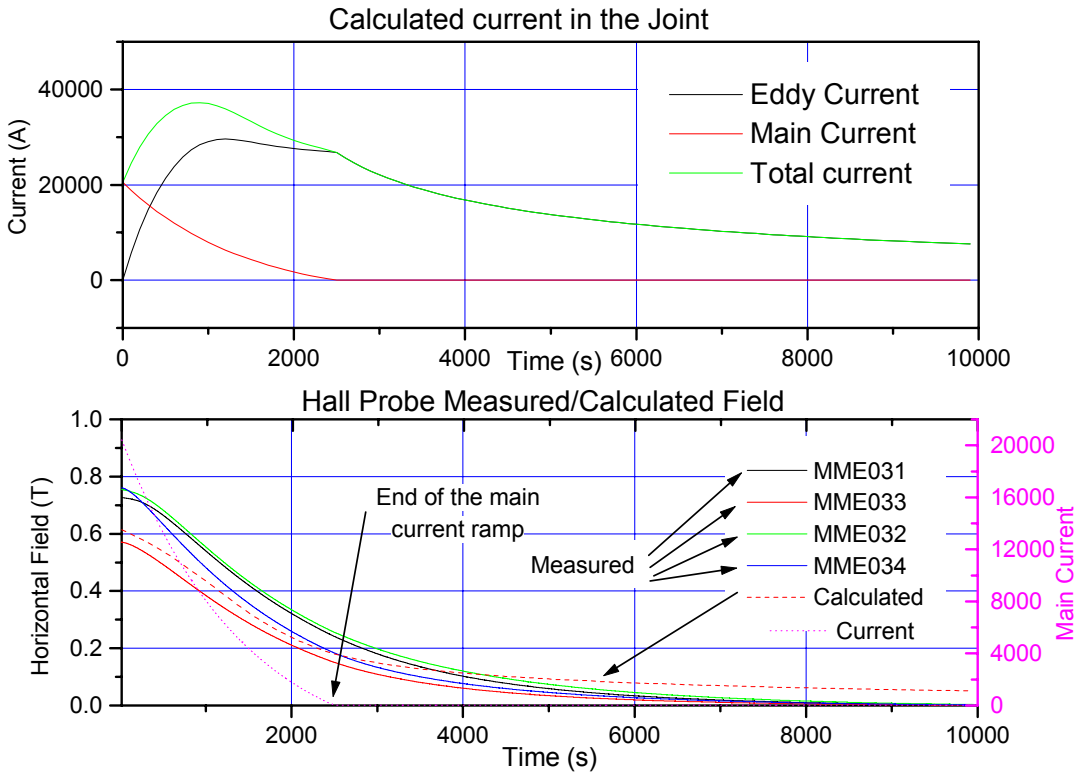

FIG. 15: Main current, calculated eddy current and total current (top). Measured field (solid lines) and calculated (dotted line) (bottom), during a magnet discharge.

As we can see, the calculated amplitude for the eddy current is about 50 kA and 30 kA for the charge or discharge of the magnet, these figures well approximate the measured values (see tables 3 and 5).

The calculated time constant τ=L/R for the current ramp up is $\tau \approx 1500$ s, while for the magnet discharge we have $\tau \approx 3800$ s

As we can see this model does not describe very well the eddy current behaviour in the joint.

6.2 More sophisticated model

A more accurate description of the eddy current in the joint can be described by another model where the joint is represented as a RL network circuit[4)].

In addition to the time constant and the amplitude of the eddy current this model provide the current distribution inside the joint.

The time constant of the eddy current, according to this model, is

$$\tau = \frac{2L}{\pi^2 R} \tag{11}$$

By substituting the numerical value we get $\tau \approx 630$ s, well in agreement with the experimental data.

As we can see the simple model can provide a good approximation for the eddy current amplitude, while fails in the estimation of the time constant.

7 COMMENTS AND SUMMARY

The data reported and the calculations carried out fully describe and characterize the interpancake joint of the Atlas B0 model coil and of the final barrel toroid, that will adopt the same solution.

We have stated that both theoretically and experimentally the eddy current can be very high, about 50kA. If we consider that the eddy current in one part of the joint adds to the main current while in the second part of the joint subtracts, being the main current about 20 kA, the total current in the joint can easily reach values of 70 kA, a value higher than the critical current for the cable considered. One question can arise: why there is not any quench in the joint ? (This fact is confirmed by the Hall probe signals).

To answer to this question we must consider the Fig. 16, where the critical current surfaces (I critical versus Field B) at different temperatures are plotted.

The field at the joint is, by far, due to the current passing through the B0 coil, and is influenced only marginally by the eddy current in the joint.

At 21 kA in the B0 coil, the field at the joint is 2.2 T (see field calculation).

According to the NbTi critical current scaling law[9)], at the temperature of 4.75 K the corresponding critical current is about 125 kA (T = 4.75 K, B = 2.2T, Ic = 125 kA); considering some incertitude on the temperature, at T = 4.9 K we find a critical current value of about 115 kA.

This explains why there was no quench at the coil joint, even when the current in the coil was ramped up relatively fast at 15A/s, the eddy current in the joint reached 50 kA, and the maximum current in the joint reached 70 kA, in one location over the 2.5 m; however this was still below the critical current which is in the range 115 -125 kA.

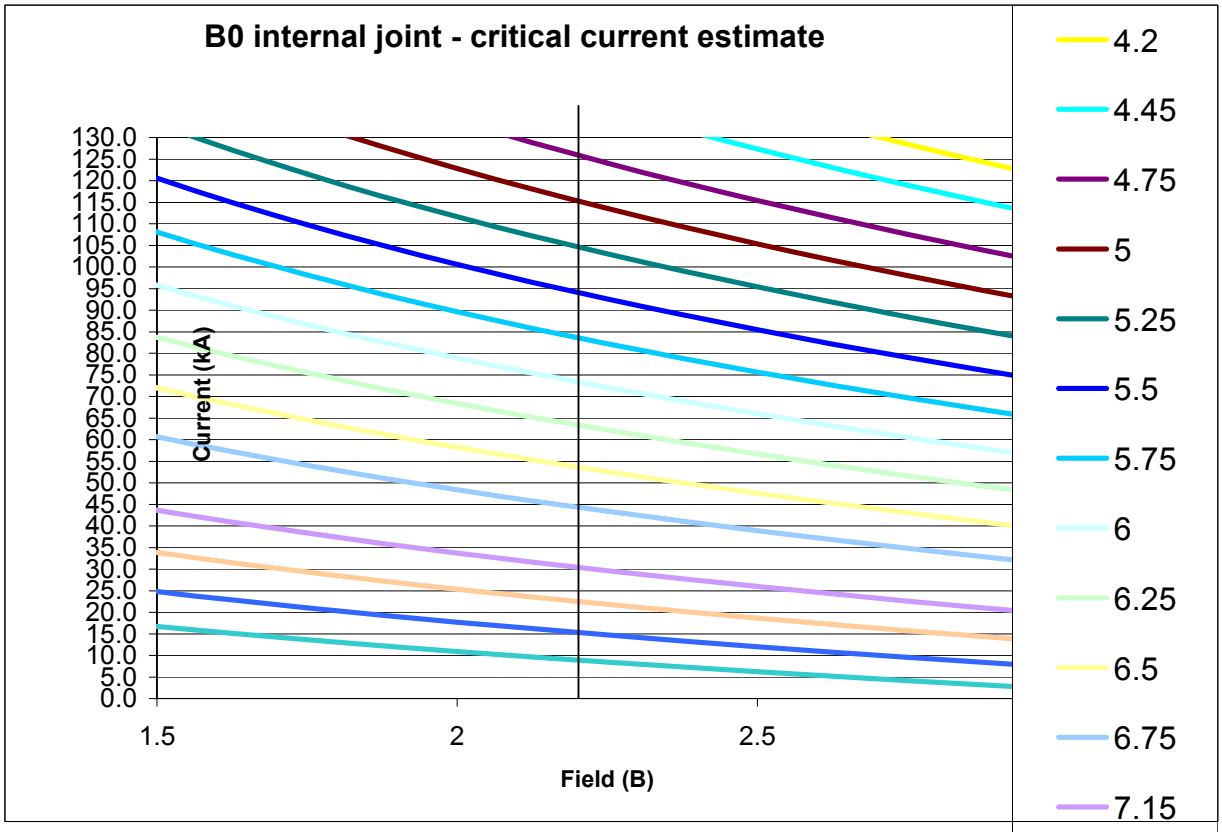

FIG. 16: Critical current surfaces (I critical versus Field B) at different temperatures.

This also proves the good design of the joint, limited to 2.5 meter length; the maximum eddy current (in one location over the joint length), scales with the square law of the joint length and i.e. a joint 3.5 meter long may have reached the critical current of 120 kA, when the current in the main B0 coil was being ramped up at 15 A/s.

In Table 8 the theoretical and experimental results are summarized.

TAB. 8: Summary of the results. The current unit is A and the time unit is s.

		Experimental				Theoretical	
		MME031	MME032	MME033	MME034	Simple	Detailed
Magnet Charge	$I_{.eddy}$ max.	~ 46700	~ 38400	~ 42000	~ 16700	~ 45000	
	τ_1	658	674	673	587	1500	608
	τ_2	674.6	693.3	662.1	575.6		
Magnet Discharge	$I_{.eddy}$ max.	~ 36000	~ 38000	~ 22500	~ 27400	~ 30000	
	τ_1	1753	2004	1647	1737	3800	1540
	τ_2	1755.8	1999.3	1643.7	1730.4		

The interpancake joint is one of the most critical part of the ATLAS barrel toroid magnets, we have seen that very high eddy current can arise in it, but the large amount of studies, both theoretical and experimental have demonstrated that no dangerous operating condition can arise during the magnet operation.

8 ACKNOWLEDGEMENTS

Our sincere acknowledgement goes to G. Rivoltella and A Paccalini for the hardware and software of the data acquisition system. Particularly appreciated are their efforts in increasing the sensitivity of the junction voltage taps channel, that allowed to discriminate between the “noise” or “real effect” discussed in section 5.2.1.

9 REFERENCES

(1) ATLAS Barrel Toroid TDR – CERN/LHCC/97 – 19 (1997).
(2) R.Berthier, F. Broggi, G.Rivoltella, A.Paccalini, “The Instrumentation of the B0 ATLAS Model Coil ”, I.N.F.N/TC-02/11, 13 Maggio 2002.
(3) F. Broggi, A. Paccalini, G. Rivoltella, "The LASA Fast Acquisition System for the B0 Diagnostics ", I.N.F.N./TC-02/21 5 Settembre 2002.
(4) G.Volpini, "A Model of the Current Distribution Inside the resistive Joints of the ATLAS Toroids",INFN/TC-00/07, 17 Maggio 2000.
(5) G.Volpini, M. Pojer, "Measurement of an Internal Joint and a Layer-to-Layer Joint as a function of the Magnetic Field ", INFN/TC-00/12, 10 Luglio 2000.
(6) C. Berriaud, “ Synthèse du Conducteur E.M.-ACS pour B0 de Fevrièr 99 (première longueur), CEA report 5 M 2 900 T –2 000 041 PA, 31/3/99.
(7) G. Baccaglioni, F. Broggi, G. Cartegni, "Design and Calibration of the Pick up coil for B0 and B00 ATLAS Model Coils", I.N.F.N./TC-02/20, 12 Luglio 2002.
(8) F.Broggi, “Pick-up Coil Quench Signal Analysis”, to be published as INFN/TC Report.
(9) A.Devred, “Review of superconducting dipole and quadrupole magnets for particle accelerators”, CEA Report DAPNIA/STCM-98-07, 1998.